Inorganic Chemistry
Article

In Search of the Bailar and Rây–Dutt Twist Mechanisms That Racemize Chiral Trischelates: A Computational Study of Sc^III, Ti^IV, Co^III, Zn^II, Ga^III, and Ge^IV Complexes of a Ligand Analogue of Acetylacetonate

Henry S. Rzepa*,† and Marion E. Cass‡

Department of Chemistry, Imperial College London, London SW7 2AZ, U.K., and Department of Chemistry, Carleton College, Northfield, Minnesota 55057

Ⓦ **This paper contains enhanced objects available on the Internet at http://pubs.acs.org/journals/inocaj.**

Two nondissociative processes, a Bailar twist that proceeds through a transition state of D_{3h} symmetry and a Rây–Dutt twist mechanism that proceeds through a transition state of C_{2v} symmetry, as well as dissociative/associative processes are potential mechanisms by which the enantiomeric forms of chiral metal trischelates can be interconverted. We have applied density functional theory to locate the stationary points for metal trischelates of a β-diketonate ligand analogue that interconvert Δ and Λ forms via one or both of these nondissociative pathways. Although many two-dimensional static representations of the Bailar and Rây–Dutt twist mechanisms can be found in the chemical literature (of the type shown in Figure 1), in this communication, we present our results in the form of interactive three-dimensional animations as a means of enhancing the scientific perception of these fluxional processes.

Introduction

Trischelates are well-known examples of metal complexes, which can exist as separate enantiomers, belonging (if appropriately substituted) to the chiral D_3 or C_3 point groups. Analyses of how such complexes can racemize via nondissociative ligand exchange were first presented in the late 1940s, although dissociative processes have long been proposed to be operative in isomerization/racemization mechanisms in complexes of kinetically labile metals. The two nondissociative pathways accepted as possible mechanisms for the racemization of D_3 metal chelates (and racemization or racemization and *facial-meridional* isomerization C_3 metal tris chelates) are the Bailar[1a] and Rây–Dutt twist mechanisms,[1b] illustrated in a two-dimensional representation in Figure 1. The Bailar twist is a trigonal twist around the real C_3 axis of a metal trischelate, and the Rây–Dutt is a twist (sometimes referred to as a rhombic twist)

around the pseudo-C_3 axis. The Bailar and Rây–Dutt twist mechanisms have been the subject of theoretical study,[1–4] experimental verification,[4–11] and computational analysis.[11,12]

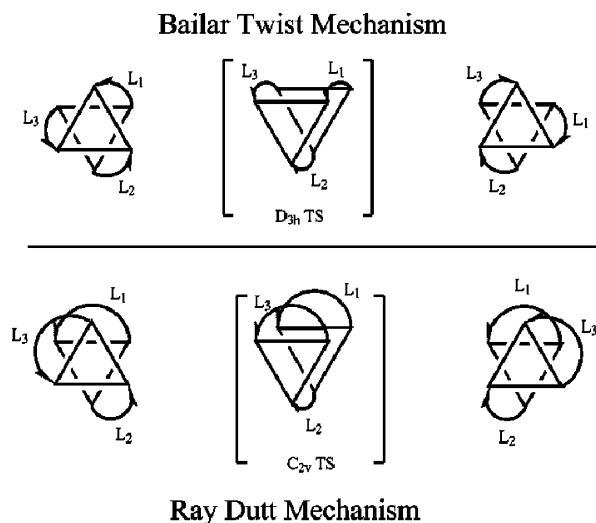In this communication, we present our results of a computational study on a series of metal trischelates of a

* To whom correspondence should be addressed. E-mail: h.rzepa@imperial.ac.uk.
† Imperial College London.
‡ Carleton College.

(1) (a) Bailar, J. C., Jr. *J. Inorg. Nucl. Chem.* **1958**, *8*, 165. (b) Rây, P.; Dutt, N. K. *J. Indian Chem.* **1943**, *20*, 81. (c) Springer, C. S.; Sievers, R. E. *Inorg. Chem.* **1967**, *6*, 852–854. (d) Brady, J. E. *Inorg. Chem.* **1969**, *8*, 1208–1209.

(2) Rodger, A.; Johnson, B. F. G. *Inorg. Chem.* **1988**, *27*, 3061–3062.
(3) Kepert, D. L. *Prog. Inorg. Chem.* **1977**, *23*, 1–65.
(4) Gordon, J. G.; Holm, R. H. *J. Am. Chem. Soc.* **1970**, *92*, 5319–5332. See also: Springer, C. S., Jr. *J. Am. Chem. Soc.* **1973**, *95*, 1459–1467.
(5) Hutchinson, J. R.; Gordon, J. G.; Holm, R. H. *Inorg. Chem. Soc.* **1971**, *10*, 1004–1017.
(6) Fay, R. C.; Piper, T. S. *Inorg. Chem.* **1964**, *3*, 348–356.
(7) Gromova, M.; Jarjayes, O.; Hamman, S.; Nardin, R.; Beguin, C.; Willem, R. *Eur. J. Inorg. Chem.* **2000**, 545–550.
(8) (a) Eaton, S. S.; Eaton, G. R.; Holm, R. H.; Muetterties, E. L. *J. Am. Chem. Soc.* **1973**, *95*, 1116–1124. (b) Eaton, S. S.; Hutchison, J. R.; Holm, R. H.; Muetterties, E. L. *J. Am. Chem. Soc.* **1972**, *94*, 6411–6426.
(9) (a) Pignolet, L. H.; Lewis, R. A.; Holm, R. H. *J. Am. Chem. Soc.* **1971**, *93*, 360–371. (b) Que, L., Jr.; Pignolet, L. H. *Inorg. Chem.* **1974**, *13*, 351–356. (c) Palazzotto, M. C.; Duffy, D. J.; Edgar, B. L.; Que, L., Jr.; Pignolet, L. H. *J. Am. Chem. Soc.* **1973**, *95*, 4537–4545.
(10) Kersting, B.; Telford, J. R.; Meyer, M.; Raymond, K. N. *J. Am. Chem. Soc.* **1996**, *118*, 5712–5721.
(11) Davis, A. V.; Firman, T. K.; Hay, B. P.; Raymond, K. N. *J. Am. Chem. Soc.* **2006**, *128*, 9484–9496.
(12) Montgomery, C. D.; Shorrock, C. J. *Inorg. Chim. Acta* **2002**, *328*, 259–262. Amati, M.; Lelj, F. *Chem. Phys. Lett.* **2002**, *363*, 451–457.

Bailar Twist Mechanism

Ray Dutt Mechanism

Figure 1. Two-dimensional illustration of the Bailar and Rây−Dutt twist mechanisms that racemize D_3 metal trischelates or isomerize C_3 metal trischelates.

simple ligand analogue of the acetonylacetonate (acac) ligand, with a focus on the following aspects of nondissociative mechanisms that racemize metal trischelates: We have applied density functional theory (DFT) computational techniques to systems that corroborate mechanistic proposals based on experimental observations, and we have presented our computational work in the form of interactive three-dimensional animations that we hope facilitate understanding.

We have previously analyzed[13] the nondissociative mechanisms that interchange apical and equatorial atoms in AEX_5 square-pyramidal molecules such as ClF_5 and IBr_5. Our analysis was considerably assisted by visual inspection of the mechanism via animation of the normal mode of the imaginary frequency of the transition state. Through visual comparison of those modes to the modes in known fluxional processes (including the Berry pseudorotation, lever, turnstile and Bartell mechanisms, which we had previously animated for pedagogic purposes[14]), we were able to identify combinations of shared characteristic motions. The hybrid motions that we identified in the apical/equatorial atom exchange of square-pyramidal molecules we termed *chimeric* pseudorotations. Here, we extend the approach of using visual three-dimensional animations to an analysis of fluxional processes in D_3 six-coordinate (octahedral) trischelates, examples of which are known for almost all transition and nontransition series metals.

In selecting metals for study, we confined ourselves here to diamagnetic species and excluded those metals where single electron-pair occupancy of degenerate (E) molecular orbital levels (at D_{3h} or D_3 symmetry) leads to Jahn−Teller-like distortions from these symmetries (e.g., Mn and Cu). We also restricted our examination of the Bailar and Rây−Dutt twist nondissociative processes to a series of metal complexes involving a simple model analogue of the β-diketonate ligand acac. The metal complexes of the β-diketonate ligands have been extensively studied; informa-

tion on the structure and reactivity[15a] as well as mechanistic studies on isomerization/racemization processes[15b] is available for comparison with our computational results. Furthermore, our model ligand, namely, the 1,3-propanedionato or malondialdehyde ligand (mda), has been previously used in computational models,[16] and one X-ray crystal structure of a $Cr(mda)_3$ complex is known.[17]

Computational Methods

In order to achieve accurate modeling of the geometry and angular behavior at the central atom, we used the correlation-consistent 5ζ basis (and in one example when the 5ζ basis failed to converge, a 4ζ basis) on this atom itself (cc-pv5Z) in combination with the *Gaussian 03* program.[18] Use of the 5ζ basis on the ligands would have been prohibitive in terms of computer time, and these were instead limited to the 6-31G(d) basis. This combination of the DFT method and basis sets has proven reliable for other atom-centered systems.[13] In two cases only, this combination yielded tiny negative force constants corresponding to out-of-plane ligand deformations, behavior that has been reported for the 6-31G-(d) basis for aromatic systems.[19] Replacing this 6-31G(d) basis with the improved cc-pVTZ basis on the ligand removes this negative force constant but at the expense of significantly increased processing time. Within this series, we have computationally characterized both the D_{3h} Bailar and C_{2v} Rây−Dutt diamagnetic transition states for the Sc^{III}, Ti^{IV}, Zn^{II}, Ga^{III}, and Ge^{IV} trisligand complexes at the B3LYP DFT level, including calculation of the Hessian second-derivative matrix, and from this, we did analysis of the transition mode and its group theoretical character. Appropriate symmetry number corrections for the entropies were included.

Results and Discussion

For each $M(mda)_3$ complex under examination ($M = Sc^{III}$, Ti^{IV}, Co^{III}, Zn^{II}, Ga^{III}, and Ge^{IV}), we computed an equilibrium
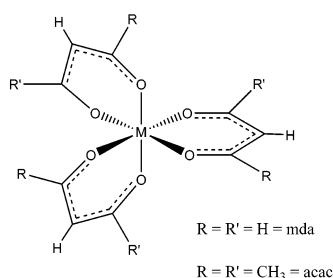
(13) Rzepa, H. S.; Cass, M. E. *Inorg. Chem.* **2006**, *45*, 3958−3963.
(14) Cass, M. E.; Hii, K. K.; Rzepa, H. S. *J. Chem. Educ.* **2006**, *83*, 336.

(15) (a) Collman, J. P. *Angew. Chem. Int. Ed.* **1965**, *4*, 132−138. Collman, J. P. *Adv. Chem. Ser.* **1963**, *37*, 78−98. (b) Fortman, J. J.; Sievers, R. E. *Coord. Chem. Rev.* **1971**, *6*, 331−375. Serpone, N.; Bickley, D. G. *Prog. Inorg. Chem.* **1972**, *17*, 391−566.
(16) Li, X.; Bancroft, G. M.; Puddephatt, R. J.; Yuan, Z.; Tan, K. H. *Inorg. Chem.* **1996**, *35*, 5040−5049.
(17) Glick, M. D.; Andrelczyk, B.; Lintvedt, R. L. *Acta Crystallogr., Sect. B: Struct. Crystallogr. Cryst. Chem.* **1975**, *31*, 916.
(18) Basis sets: Balabanov, N. B.; Peterson, K. A. *J. Chem. Phys.* **2005**, *123*, 064107/1−064107; **2006**, *125*, 074110. Frisch, M. J.; Trucks, G. W.; Schlegel, H. B.; Scuseria, G. E.; Robb, M. A.; Cheeseman, J. R.; Montgomery, J. A., Jr.; Vreven, T.; Kudin, K. N.; Burant, J. C.; Millam, J. M.; Iyengar, S. S.; Tomasi, J.; Barone, V.; Mennucci, B.; Cossi, M.; Scalmani, G.; Rega, N.; Petersson, G. A.; Nakatsuji, H.; Hada, M.; Ehara, M.; Toyota, K.; Fukuda, R.; Hasegawa, J.; Ishida, M.; Nakajima, T.; Honda, Y.; Kitao, O.; Nakai, H.; Klene, M.; Li, X.; Knox, J. E.; Hratchian, H. P.; Cross, J. B.; Bakken, V.; Adamo, C.; Jaramillo, J.; Gomperts, R.; Stratmann, R. E.; Yazyev, O.; Austin, A. J.; Cammi, R.; Pomelli, C.; Ochterski, J. W.; Ayala, P. Y.; Morokuma, K.; Voth, G. A.; Salvador, P.; Dannenberg, J. J.; Zakrzewski, V. G.; Dapprich, S.; Daniels, A. D.; Strain, M. C.; Farkas, O.; Malick, D. K.; Rabuck, A. D.; Raghavachari, K.; Foresman, J. B.; Ortiz, J. V.; Cui, Q.; Baboul, A. G.; Clifford, S.; Cioslowski, J.; Stefanov, B. B.; Liu, G.; Liashenko, A.; Piskorz, P.; Komaromi, I.; Martin, R. L.; Fox, D. J.; Keith, T.; Al-Laham, M. A.; Peng, C. Y.; Nanayakkara, A.; Challacombe, M.; Gill, P. M. W.; Johnson, B.; Chen, W.; Wong, M. W.; Gonzalez, C.; Pople, J. A. *Gaussian 03*, revision D.02; Gaussian, Inc.: Wallingford, CT, 2004.
(19) Loran, D.; Simmonett, A. C.; Leach, F. E.; Allen, W. D.; Schleyer, P. v. R.; Schaefer, H. F. *J. Am. Chem. Soc.* **2006**, *128*, 9342−9343.

Table 1. List of Web Enhanced Objects for Visualization of Equilibrium and Transition-State Geometries[a]

web enhanced object	description
1	Structural information for the computed structures of ScL_3, $[TiL_3]^+$, CoL_3, $[ZnL_3]^-$, GaL_3, and $[GeL_3]^+$ (L = mda)
2	Contrasting the computed equilibrium geometries for ScL_3, $[TiL_3]^+$, CoL_3, $[ZnL_3]^-$, GaL_3, and $[GeL_3]^+$ (L = mda) with the known crystal structures for $Sc(acac)_3$, $[Ti(acac)_3]ClO_4$, $Co(acac)_3$, $Zn_3(acac)_6$, $Ga(acac)_3$, and $[Ge(acac)_3]ClO_4$
3	Computed energies and imaginary frequencies for all species examined in this study
4	Bailar twist for GaL_3 (L = mda)
5	Rây−Dutt mechanism for GaL_3 (L = mda)
6	Five-coordinate intermediate for CoL_3 (L = mda)

[a] Viewing the web enhanced object requires Java (version 1.1 or greater) to be installed, together with a browser that supports this Java; we recommend, e.g., Firefox.

Figure 2. Tris metal complex of a β-diketonate ligand. Abbreviations for ligands used or referred to in this study: acetylacetonate, acac; malondialdehyde, mda; 1-phenyl-5-methylhexane-2,4-dione, pmhd; 5-methylhexane-2,4-dione, mhd; trifluoroacetylacetonate, tfac; benzoylacetonate, bzac (R = R′ = CH_3); triacetonylmethanide-d_3, triac-d_3.

geometry (presented as web enhanced objects; see Table 1) and then searched for a transition state of D_{3h} (Bailar) or C_{2v} (Rây−Dutt) symmetry.

All of the computed equilibrium geometries for the $M(mda)_3$ complexes have D_3 symmetry (see Figure 2 for the general structure and Ⓦ web enhanced object 1 for a three-dimensional interactive view of each computed structure and a listing of the relevant bond distances and angles). The total energy as well as the free energy corrected for zero-point energies and entropy are reported in web enhanced object 3 for each structure. The computed structures compare favorably to the known structure of $Cr(mda)_3$,[17] also shown in web enhanced object 1. In addition, a comparison of the structural properties of each computed $M(mda)_3$ complex to that of a reported X-ray crystal structure for the corresponding $M(acac)_3$ analogue of the same metal ion[20] illustrates how well mda mimics the acac ligand (see Ⓦ web enhanced

(20) (a) Anderson, J. J.; Neuman, M. A.; Melson, G. A. *Inorg. Chem.* **1973**, *12*, 927−930. (b) Filgueiras, C. A. L.; Horn, A., Jr.; Howie, R. A.; Skakle, J. M.; Wardell, J. L. *Acta Crystallogr., Sect. E: Struct. Rep. Online* **2001**, *57*, m157−m158. (c) Kriger, G. J.; Reynhardt, E. C. *Acta Crystallogr., Sect. B: Struct. Crystallogr. Cryst. Chem.* **1974**, *30*, 822−824. (d) Bennett, M. J.; Cotton, F. A.; Eiss, R. *Acta Crystallogr., Sect. B: Struct. Crystallogr. Cryst. Chem.* **1968**, *24*, 904−913. (e) Dymock, K.; Palenik, G. L. *Acta Crystallogr., Sect. B: Struct. Crystallogr. Cryst. Chem.* **1974**, *30*, 1364−1366. (f) Thewalt, U.; Adam, T. Z. *Naturforsch., B: Chem. Sci.* **1978**, *33*, 142. (g) Ito, T.; Toriumi, K.; Ueno, F. B.; Saito, K. *Acta Crystallogr., Sect. B: Struct. Crystallogr. Cryst. Chem.* **1980**, *36*, 2998.

Table 2. Calculated Activation Parameters[a] at the B3LYP/Gen[b] Level

complex	$\Delta G^{\ddagger}_{298}$, kcal mol^{-1}	$\Delta H^{\ddagger}$, kcal mol^{-1}	$\Delta S^{\ddagger}_{298}$, cal mol^{-1} K^{-1}	imaginary modes, cm^{-1}
	$Sc^{III}(mda)_3$			
Rây−Dutt	7.3	5.1	−7.3	60i (A_2)
Bailar	7.7	5.5	−7.3	45i (A_1'')
	$[Ti^{IV}(mda)_3]^+$			
Rây−Dutt	8.7	6.1	−9.6	48.1i (A_2)
Bailar	9.5	7.5	−8.1	68.4i (A_1'')
	$[Zn^{II}(mda)_3]^-$			
Rây−Dutt	10.0	9.0	−3.6	58i (A_2)
Bailar	10.8	10.3	−1.6	71i (A_1'')
	$Ga^{III}(mda)_3$			
Rây−Dutt	19.3	18.6	−2.4	85i (A_2)
Bailar	20.6	20.6	0.01	45i (A_1'')
	$[Ge^{IV}(mda)_3]^+$			
Rây−Dutt	29.7, 28.9^c	30.1, 29.3^c	−1.8, −1.9^c	109.3, 108.1^ci (A_2)
Bailar	32.2, 30.0^c	32.6, 31.4^c	−1.0^c	123.2, 122.7^ci (A_1'')

[a] Free energy corrected for zero-point energies and entropy. [b] Basis set: cc-pV5Z(5d,7f) on the metal center;[13] 6-31G(d) on the ligands. A more extensive table of the energies and computational parameters can be found in Ⓦ web enhanced object 3. [c] cc-pV5ζ on central atom; cc-pVTZ on ligands.

object 2 for the structural comparisons). Each mda ligand, like the acac ligand, forms a planar, six-atom metal−chelate ring and shows significant delocalization over the C−O and C−C bonds. M−O, C−O, and C−C bond lengths as well as O−M−O intraligand bite angles (listed in web enhanced object 2) are consistent within each pair of $M(mda)_3$/$M(acac)_3$ structures.

We computationally characterized a transition state of D_{3h} symmetry and of C_{2v} symmetry for each of the Sc^{III}, Ti^{IV}, Zn^{II}, Ga^{III}, and Ge^{IV} species. Computed energies are given in Table 2. The results, as well as a discussion of how our computational results compare to published mechanistic studies, are presented individually vida infra for each species. In contrast to the results for Sc^{III}, Ti^{IV}, Zn^{II}, Ga^{III}, and Ge^{IV}, we were unable to locate a transition state of D_{3h} or C_{2v} symmetry for the Co^{III} species. A stationary state of C_{2v} symmetry collapsed to yield a five-coordinate intermediate (see the discussion below), consistent with the proposal by Holm and co-workers that cobalt(III) trischelates of examined β-diketonate ligands exhibited behavior characteristic of isomerization/racemization through a dissociate mechanism proceeding through a five-coordinate species.[4]

Given that metal acetylacetonate complexes have C−O and C−C bond lengths consistent with delocalized electron density and given that the $M(acac)_3$ complexes undergo reactions normally associated with aromatic compounds such as electrophilic aromatic substitution, we calculated the nucleus-independent chemical shift (NICS) value at and above the center of the metal−mda ring in each structure to ascertain whether this was useful in understanding the aromaticity in these molecules. The NICS(1) and/or NICS(2) values (1 and 2 Å, respectively, above the centroid of a ring) are useful in predicting the aromaticity in organic and organometallic complexes.[21] More recently, researchers have begun to calculate NICS(1) and/or NICS(2) to estimate the

aromaticity of coordination complexes.[22] All of the ground-state geometries that we computed in this study gave NICS-(2) values close zero (±2 ppm), indicative of nonaromatic rings [NICS(1) values show slightly more contribution/contamination from local metal effects and the σ-derived ring currents]. Apparently, all of the empty orbitals available on all of the metals used in this study are sufficiently mismatched in energy for effective π delocalization.

$Sc^{III}L_3$. The D_{3h} transition state for the Sc(mda)$_3$ complex has a barrier ($\Delta G^{\ddagger} = 7.7$ kcal mol^{-1}, 32.1 kJ mol^{-1}) similar to that of the C_{2v} transition state ($\Delta G^{\ddagger} = 7.3$ kcal mol^{-1}, 29.3 kJ mol^{-1}). For each of the two computed transition states, a single imaginary frequency was found: $60i$ cm^{-1} for the D_{3h} Bailar transition state (with an A_1'' irreducible representation) and $45i$ cm^{-1} for the C_{2v} Râmy−Dutt transition state (with an A_2 irreducible representation). With such low-energy barriers for both transition states, these Sc^{III} complexes would be predicted to thermally racemize well below room temperature (although dissociative pathways may well also occur in solution, and we have not computationally explored these types of pathways). Animations of the Bailar and Râm−Dutt twist mechanisms for the racemization of Sc(mda)$_3$ are visually identical with that of Ga(mda)$_3$, shown in ⓦ web enhanced object 4 and ⓦ web enhanced object 5, respectively. An experimental study found that the Sc^{III} triscomplex of the 1-phenyl-5-methylhexane-2,4-dione (pmhd) β-diketonate ligand (Figure 1; R = CH(CH$_3$)$_2$ and R$'$ = CH$_2$C$_6$H$_5$) exhibited fast fluxional behavior in the ^{1}H NMR spectrum in chlorobenzene and at temperatures as low as -95 °C in dichloromethane.[5] At significantly higher temperatures (60° in chlorobenzene, and 40° in chloroform), addition of alternatively substituted scandium β-diketonates or free alternatively substituted β-diketonate ligands resulted in mixed-ligand complexes indicative of intermolecular exchange.[5]

$[Ti^{IV}L_3]^+$. The Ti^{IV} complex is very similar to the Sc^{III} system; the only significant difference is that the loss of entropy at either of the two transition states is slightly greater, indicating tighter binding for the cationic system. Again, the C_{2v} transition state has a slightly lower barrier ($\Delta G^{\ddagger} = 8.7$ kcal mol^{-1}) than that of the D_{3h} transition state ($\Delta G^{\ddagger} = 9.5$ kcal mol^{-1}). Imaginary frequencies for each computed transition state are reported in Table 2. Animations of the imaginary frequencies for the Bailar and Râm−Dutt twist mechanisms are visually identical with those for the mda complexes of Sc^{III}, Ti^{IV}, Ga^{III}, and Ge^{IV}.

Co(III)L_3. True D_{3h} and C_{2v} transition states for the tris-(mda) complex of Co^{III} were not locatable. The stationary state of C_{2v} symmetry at 60.4 kcal mol^{-1} above the equilibrium D_3 geometry had B_2 and A_2 imaginary modes. While the latter is the Râm−Dutt mode, the former corresponds to asymmetric Co−O stretching of the unique ligand.

Following the Râm−Dutt mode results in complete fission of one Co−O bond to give a five-coordinate intermediate at 39.4 ($\Delta G = 34.5$) kcal mol^{-1} above the equilibrium D_3 geometry (using a 4ζ basis on the metal; the corresponding 5ζ basis proved unconvergeable). This corresponds to a dissociative process for Λ and Δ interconversion, albeit one that is only accessible with high-energy input. This intermediate is shown in ⓦ web enhanced object 6. The absence of a low-energy pathway for thermal isomerization is consistent with the experimental observation that the Λ and Δ forms of the analogous Co(acac)$_3$ complex are isolable and stable to racemization at room temperature.[15] Furthermore, an extensive mechanistic study based on an analysis of the temperature-dependent reaction rates of isomerization and racemization for Co(mhd)$_3$ (Figure 1; R = CH(CH$_3$)$_2$ and R$'$ = CH$_3$) monitored by ^{1}H NMR and circular dichroism spectroscopy indicates that this process involves bond rupture to generate a five-coordinate species.[4] The barriers for these isomerization and racemization processes (tabulated in Table 3 for comparison, along with values for isomerization and racemization in other similar cobalt(III) β-diketonates[4−6]) agree reasonably well with theory. It is noteworthy, however, that our calculated $\Delta S^{\ddagger}$ for the dissociative process (+13.7 cal K^{-1} mol^{-1}) is rather larger than that derived from kinetic measurement ($\sim+6−9$ cal K^{-1} mol^{-1}), which implies that, in practice, the five-coordinate intermediate may be more highly solvated than the D_3 ground state.
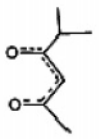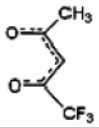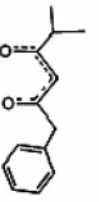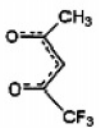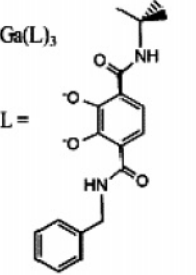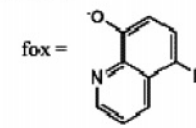
$[Zn^{II}L_3]^-$. The D_{3h} and C_{2v} transition states for the [Zn(mda)$_3$]$^-$ anion have relatively low and very similar energy barriers (for the D_{3h} Bailar transition state, $\Delta G^{\ddagger} = 10.8$ kcal mol^{-1}, and for the C_{2v} transition state, $\Delta G^{\ddagger} = 10.0$ kcal mol^{-1}). With such low-energy barriers, these Zn^{II} complexes would be expected to racemize well below room temperature. For each of the two computed transition states, a single imaginary frequency was found: $70.7i$ cm^{-1} for the Bailar transition state of D_{3h} symmetry and $58.2i$ cm^{-1} for the Râm−Dutt transition state of C_{2v}. Animations of the Bailar and Râm−Dutt twist mechanism for the racemization of the Zn complex again are visually identical with that of Ga-(mda)$_3$, shown in web enhanced objects 4 and 5, respectively.

Ga$^{III}L_3$. The results of our computational study are perhaps the most interesting for the Ga^{III} species of the mda ligand. As with the Sc^{III} and Zn^{II} complexes, the D_{3h} and C_{2v} transition states have fairly similar energy barriers ($\Delta G^{\ddagger} = 20.6$ kcal mol^{-1} for the D_{3h} Bailar transition state and $\Delta G^{\ddagger} = 19.3$ kcal mol^{-1} for the C_{2v} Râm−Dutt transition state). Unlike the Zn^{II} and Sc^{III} homologues, however, the energy barriers fall within a range that is both high enough to prevent immediate and complete racemization under reasonable experimental conditions and low enough to access without thermal degradation. In an experimental study of line broadening in the resonances of the Ga(pmhd)$_3$ complex measured between 31 and 105 °C, the fluxional processes were determined to involve both isomerization and inversion of the absolute configuration.[5] Furthermore, experiments carried out with the similar Ga(triac-d_3)$_3$ complex measured bond rupturing linkage isomerization reactions to proceed at $^1/_{800}$ of the reaction rate of the isomerization/racemization,

(21) Schleyer, P. v. R.; Maerker, C.; Dransfeld, A.; Jiao, H.; van Eikema Hommes, N. J. R. *J. Am. Chem. Soc.* **1996**, *118*, 6317−6318. For a review, including organometallic systems, see: Schleyer, P. v. R.; Chen, Z.; Wannere, C.; Corminboeuf, C.; Puchta, R. *Chem. Rev.* **2005**, *105*, 3842−3888.

(22) Makedonas, C.; Mistopoulou, C. A. *Eur. J. Inorg. Chem.* **2006**, 2460−2468.

Table 3. Experimentally Measured Activation Parameters for Relevant Systems

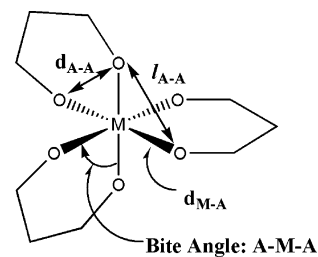| System	Processes Observed	Reported Activation Energies are in kcal mol^{-1}, entropies in cal K^{-1} mol^{-1}	Comments	Ref
Co(III) Systems				
Co(mhd)$_3$ mhd ≡	Co(mhd)$_3$ Isomerization *cis-trans* *trans-cis* *Racemization* for *cis* for *trans*	$\Delta G^{\ddagger}_{Calc\ 293K} = 30.4$, $\Delta H^{\ddagger} = 32.9$, $\Delta S^{\ddagger} = 8.7$ $\Delta G^{\ddagger}_{Calc\ 293K} = 30.8$, $\Delta H^{\ddagger} = 32.6$, $\Delta S^{\ddagger} = 6.3$ $\Delta G^{\ddagger}_{Calc\ 293K} = 29.4$, $\Delta H^{\ddagger} = 29.9$, and $\Delta S^{\ddagger} = 1.5$ $\Delta G^{\ddagger}_{Calc\ 293K} = 29.6$, $\Delta H^{\ddagger} = 31.6$, and	**Bond Rupture Mechanism (proceeding through a five coordinate intermediate) is proposed** Measurements of temperature dependent rates using proton NMR and CD	4
		$\Delta S^{\ddagger} = 6.8$	Spectroscopy Solvent: Chlorobenzene	
Co(tfac)$_3$ tfac ≡	Co(tfac)$_3$ Isomerization	$\Delta G^{\ddagger}_{455K} = 26.8$, $\Delta S^{\ddagger} = 8.6$	Barrier Determined from Coalescence of ^{19}F NMR Signals Solvent: Chloroform	6
Ga(III) Systems				
Ga(pmhd)$_3$ pmhd ≡	Ga(pmhd)$_3$ Isomerization/Racemization	$\Delta G^{\ddagger}_{Calc\ 293K} = 18.6$, $\Delta H^{\ddagger} = 19.4$, and $\Delta S^{\ddagger} = 2.9$	**Non-dissociative Twist Mechanisms are Proposed to be most consistent with experimental observations** Measurements by proton NMR Analysis of Temperature Dependent Line Broadening Solvent: Chlorobenzene	5
Ga(tfac)$_3$ tfac ≡	Ga(tfac)$_3$ Isomerization/Racemization	$\Delta G^{\ddagger}_{335K} = 17.5$	Barrier Determined from Coalescence of ^{19}F NMR Signals Solvent: Chloroform	6
Ga(L)$_3$ L ≡	Ga(L)$_3$ Intramolecular Racemization Intramolecular Isomerization	$\Delta G^{\ddagger}_{295} = 14$ kcal/mol (60 kJ/mol) in D$_2$O $\Delta G^{\ddagger}_{327} = 16$ kcal/mol (67 kJ/mol) in DMSO-d^6 Barrier for Isomerization (Rây-Dutt) is larger than that for Racemization Computed Barrier for the Bailar Twist: $\Delta E = 12.7$ kcal/mol (53 kJ/mol) Computed Barrier for the Rây-Dutt: $\Delta E = 16$ kcal/mol (67 kJ/mol)	**The Bailar Twist was shown both experimentally and computationally to be the dominant process** No observed ligand exchange was used to confirm that racemization processes are intramolecular Barrier Determined Experimentally from Coalescence and Line Shape Analysis of VT ^{1}H NMR	10 11
Ga(fox)$_3$ fox ≡	Ga(fox)$_3$ Isomerization/Racemization Bailar ≈ Rây-Dutt	$\Delta G^{\ddagger}_{293K} = 14.4$, $\Delta H^{\ddagger} = 16.9$, and $\Delta S^{\ddagger} = 6.7$	**Proposed Mechanism: Bailar and Rây-Dutt** Measurements Temperature Dependent Line Broadening of ^{19}F-NMR signals and use of 2D EXSY ^{19}F-NMR Cross Peak Intensities Solvent: DMF	7

allowing the authors to rule out a fluxional process involving bond rupture. Collectively, these experimental observations led the authors to support a fluxional twist mechanism that occurred along the real C_3 (Bailar twist) and pseudo C_3 (Râ-Dutt) axes.[5] The barrier for the collective twist processes is reported in Table 3 for comparison along with that for Ga(tfac)$_3$,[6] bearing in mind that the fluorinated β-diketonates have been reported to have lower barriers for isomerization/racemization reactions than their alkyl analogues.[5]

In a recent set of experiments, Raymond and his co-workers were able to experimentally observe the racemization of Δ and Λ-*trans*-tris(2,3-dihyroxy-*N*-*tert*-butyl-*N'*-benzyl-terephthalamide)gallium(III) via variable-temperature ^{1}H NMR. The experimentally determined activation barrier for the Bailar twist [$\Delta G^{\ddagger}_{295} = 14$ kcal mol^{-1} (60 kJ mol^{-1}) in D$_2$O] is lower than that observed for isomerization processes that would proceed via a Râ-Dutt mechanism.[10] Computational studies confirmed the Bailar twist to have a lower activation barrier relative to the Râ-Dutt twist for this GaL$_3$ complex and give excellent agreement with experimentally determined results.[11]

In another recent publication, two-dimensional exchange spectroscopy (EXSY) and dynamic ^{19}F NMR were used to examine the fluxional processes for the *meridional* isomer of the Ga^{III} complex of the unsymmetrical chelate 5-fluoro-8-hydroxyquinoline (fox). The minor facial (cis) isomer has C_3 symmetry. Line-shape analysis for the ^{19}F NMR signals undergoing exchange, as well as cross-peak intensities in the two-dimensional EXSY spectrum, were used to calculate the activation barriers for twist mechanisms. The authors suggest that two nondissociative mechanisms (Râ-Dutt and Bailar) have identical values for $\Delta H^{\ddagger}$ (Table 3),[7] differing only in $\Delta S^{\ddagger}$ effectively corresponding to a rate difference of 2.1. Their experiment proves conclusively that a Râ-Dutt mechanism *must* operate; their inference of an (equal) kinetic contribution from a Bailar mechanism is less direct.[7]

Our computational results on Ga(mda)$_3$ compare favorably to the experimental results discussed above. [See web enhanced objects 4 and 5 for visualizations of the Bailar and Râ-Dutt twist mechanisms for Ga(mda)$_3$.] A possible exception is the computed entropy of activation. Whereas the measured values are positive ($+3$–7 cal K^{-1} mol^{-1}), the computed values are somewhat less (Râ-Dutt, -2.4 cal K^{-1} mol^{-1}; Bailar, 0.0 cal K^{-1} mol^{-1}). We also note that, throughout the series Sc^{III}–Co^{III}–Zn^{II}–Ga^{III}, the free-energy barrier for the Râ-Dutt process is uniformly less than that for the Bailar process. In the specific case of Ga^{III}, the value of $\Delta G^{\ddagger}$(Râ-Dutt) $- \Delta G^{\ddagger}$(Bailar) is about 1.3 kcal mol^{-1}, which corresponds to a rate factor of about 9 less for the Bailar process and therefore suggests a possibility that there is, in fact, little or no contribution from the Bailar process for the Ga^{III} fluxional process for this β-diketonate complex.

[Ge^{IV}L$_3$]$^+$. The cationic Ge^{IV} system completes the trend, revealing the largest barriers in the series. The imaginary modes also have the largest values in the series (see Table 2). Raymond and co-workers similarly found that the computed and experimentally determined barriers for intramolecular rearrangement in the trischelates of substituted

Normalized bite = $b = d_{A-A} / l_{A-A}$

Figure 3. Parameters measured to predict the relative magnitude of the barriers to intramolecular rearrangement and the relative barriers to Bailar versus Râ-Dutt twist mechanisms: b = normalized bite size = distance between the two ligating atoms within the same chelate ring (d_{A-A}) divided by the metal–donor atom bond distance (d_{M-A}). Some analyses examine the ratio of d_{A-A} to l_{A-A} (the ligand-to-ligand hard-sphere distance) as a predictor of the preferred intramolecular rearrangement mechanism.

catecholates were the largest for Ge^{IV} within the examined series of Ti^{IV}, Ga^{III}, and Ge^{IV} complexes.[11]
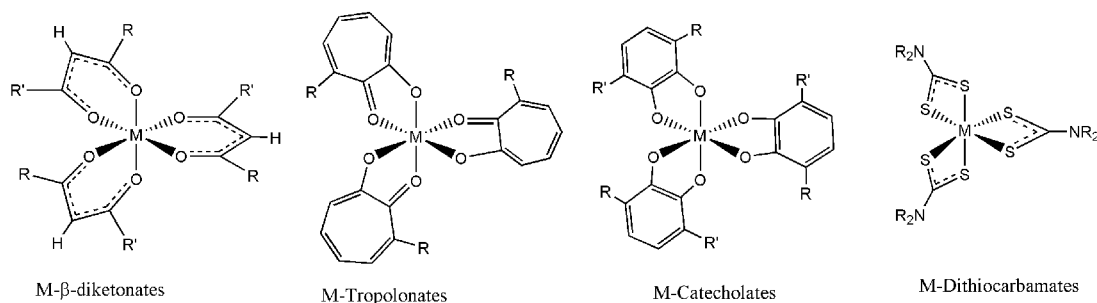
Trends and Comparison to Predicted Results

Theory predicts that, because the "normalized bite" (b; see Figure 3) of a metal chelate complex decreases (either within a series of metal–ligand complexes of the same metal or within a series of metal–ligand complexes of the same ligand), intramolecular mechanisms for racemization/isomerization should become more favorable.[3,11] Complexes with smaller b values for the ground-state structures are distorted toward the trigonal-prismatic transition state of D_{3h} or C_{2v} symmetry, therefore lowering the activation barrier for the intramolecular rearrangement. The normalized bite size has been reported to be a better predictor of the barrier to intramolecular rearrangement because the distance between ligating atoms within a given chelate ring (d_{A-A}) is *not* invariant across a series of metal complexes of that same ligand.[3,11] In addition, it has been proposed that metal ions with empty or partially empty d orbitals (e.g., V^V, Ti^{IV}, V^{III}, etc.) are favorably distorted toward trigonal-prismatic geometries to optimize ligand-to-metal σ and π bonding.[11] These metal complexes have lower barriers to intramolecular isomerization, which is correctly predicted by the normalized bite size (b) and incorrectly predicted by the metal-to-donor atom (d_{M-A}) bond distance alone.

Theory also predicts that the Bailar twist intramolecular rearrangement mechanism has a lower activation barrier relative to the Râ-Dutt mechanism as b decreases across a series of metal–ligand complexes. Three sets of authors give different values for b as a cutoff for when the Bailar twist becomes the predominant intramolecular rearrangement mechanism. Beguin states that "when this value is less than 1.5, the Bailar twist is energetically preferred over a Râ-Dutt twist."[7] Montgomery reports that "compounds with a relatively small b value ($b/M - L < 2^{1/2}$) will choose the Bailar Twist over the Râ-Dutt",[12] and Kepert's original work proposes that in complexes of "ligands with normalized bites below approximately 1.3 ... the twist about the C_3 axis will be favored."[3]

Rodger and Johnson developed a modified form of Kepert's geometric analysis to predict relative rates and

Scheme 1

M-β-diketonates   M-Tropolonates   M-Catecholates   M-Dithiocarbamates

preferred reaction pathways for these intramolecular processes. Like Kepert, they examined the unfavorable energy change associated with metal−ligand ($d_{M−A}$) bond stretching that must occur to pass through the transition state, offset by a smaller energy change in dispersion stabilization from the interaction of ligand nearest-neighbor atoms to predict which nondissociative mechanism is more favorable. A value is calculated for the ratio of the distance between two ligating atoms within the same chelate ring ($d_{A−A}$) to the ligand-to-ligand hard-sphere distance [$l_{A−A}$, where a "reasonable estimate of l can be made by measuring the shortest nearest neighbor distance of the reactant (usually between two atoms related by the 3-fold axis of the complex)"[2]] (Again see Figure 3.) A molecule with a small value of the ratio of $d_{A−A}/l_{A−A}$ (near 0.5) is predicted to proceed via a Bailar twist, whereas a molecule with a large ratio of $d_{A−A}/l_{A−A}$ (near 1.5) will proceed via a Rây−Dutt twist mechanism. A molecule with an intermediate ratio of $d_{A−A}/l_{A−A}$ (near 1.0) will proceed through either mechanism "as there will be little difference between the energies of the two structures".[2] Thus, two schemes have been put forward to assess the reaction rates and pathways in the fluxional processes of metal trischelates; Kepert compares values of b (the normalized

bite), and Rodger and Johnson compare values of $d_{A−A}/l_{A−A}$. Because different authors reference different assessment schemes, we have included both in order to compare our computational data to experimental results and to other computational results.

A number of studies have been published on the intramolecular rearrangements of metal complexes of the $β$-diketonates, tropolonates, catecholates, and dithiocarbamates (Scheme 1). Consistent with theory, general trends show that $β$-diketonates have larger normalized bite values (b near 1.4) and have slower rates of racemization/isomerization than the tropolonates (with b values near 1.3) or catecholates (with b values ranging from 1.26 to 1.34). The dithiocarbamates (with b values near 1.2) are experimentally observed to have the fastest rates of racemization/isomerization within this series chosen for comparison.

Some experimental studies have been able to distinguish between Bailar and Rây−Dutt twists and, as Raymond points out, this "experimental differentiation ... can be difficult."[11] In 1996 and 2006, the Raymond group reported experimental findings that showed a preference of a Bailar twist over the Rây−Dutt twist in the intramolecular rearrangements of metal complexes of substituted catecholates (these complexes

Table 4

system	$\Delta G^{\ddagger}$, kcal mol^{-1}	ionic radius^a (CN = 6), Å	crystal radius^a (CN = 6), Å	bite angle,^{b} deg	d_{M-O},^{b} Å	d_{A-A},^{b} Å	l_{A-A},^{b} Å	d_{A-A}/l_{A-A}	normalized bite^b d_{A-A}/d_{M-O}	Δd_{M-O} (TS D_3), Å
Sc^{III} D_3 equil geom		0.745	0.885	81.73	2.105	2.754	3.016	0.913	1.31	
Sc^{III} Bailar	7.7	0.745	0.885		2.113					0.008
Sc^{III} Rây−Dutt	7.3	0.745	0.885		2.103, 2.126, ave^c = 2.111					−0.002, 0.021, ave^c = 0.005
Ti^{IV} D_3 equil geom		0.605	0.745	83.41	1.958	2.605	2.773	0.940	1.33	
Ti^{IV} Bailar	9.5	0.605	0.745		1.971					0.013
Ti^{IV} Rây-Dutt	8.7	0.605	0.745		1.961, 1.983, ave^c = 1.969					0.003, 0.025, ave^c = 0.011
Co^{III} D_3 equil geom		0.545	0.685	96.31	1.902	2.834	2.635	1.08	1.49	
Zn^{II} D_3 equil geom		0.74	0.88	88.34	2.115	2.948	2.995	0.984	1.39	
Zn^{II} Bailar	10.8	0.74	0.88		2.141					0.026
Zn^{II} Rây−Dutt	10.0	0.74	0.88		2.128, 2.167, ave^c = 2.141					0.013, 0.052, ave^c = 0.026
Ga^{III} D_3 equil geom		0.62	0.76	91.42	1.978	2.832	2.768	1.023	1.43	
Ga^{III} Bailar	20.6	0.62	0.76		2.009					0.031
Ga^{III} Rây−Dutt	19.3	0.62	0.76		1.998, 2.024, ave^c = 2.007					0.020, 0.046, ave^c = 0.029
Ge^{IV} D_3 equil geom		0.53	0.67	93.38	1.891	2.752	2.626	1.048	1.46	
Ge^{IV} Bailar	32.2	0.53	0.67		1.933					0.042
Ge^{IV} Rây−Dutt	29.7	0.53	0.67		1.924, 1.948, ave^c = 1.932					0.033, 0.057, ave^c = 0.041

^{a} Shannon, R. D. *Acta Crystallogr., Sect. A* **1976**, *32*, 751−767. ^{b} Distances and angles were measured in Gaussview from the M(mda)$_3$ Gaussian output files. (Also see web enhanced object 1 for M(mda)$_3$ structures and web enhanced object 2 for structural comparisons to the known M(acac)$_3$ crystal structures.) ^{c} Each Rây−Dutt transition state has two four short and two longer M−O distances. The average is taken over all six distances.

have b values ranging from 1.26 to 1.34.[10,11] Their results were supported by computation of the activation barriers for the different twist mechanisms.[11] Earlier, an experimental study of racemization/isomerization rates for metal complexes of tropolonate ligands (b near 1.3) showed a low-temperature racemization process to be the most consistent with a Bailar twist and a higher temperature process correlated to isomerization via a Rây−Dutt mechanism.[8a]

The normalized bite for our computed equilibrium geometry mda complexes as well as the ratios of d_{A-A}/l_{A-A} and the difference in metal−ligand bond distances between the equilibrium geometry and computed transition states (Δd_{M-A}) are presented in Table 4. We observe that, as the normalized bite increases, the activation barriers for both the Bailar and Rây−Dutt twist mechanisms increase and are larger than those observed for metal complexes of the tropolonates, catecholates, or dithiocarbamates with smaller values of b. Our computed activation barriers indicate that our model complexes favor the Rây−Dutt twist over the Bailar twist, although the two mechanisms have similar energy barriers as predicted by theory (with d_{A-A}/l_{A-A} values near 1.0 and relatively large values of the normalized bite that are near or greater than 1.3).[2,3] The computed change in the metal−ligand bond distance (Δd_{M-A}) for the molecule to move through the transition state is smaller for the Rây−Dutt twist over the Bailar twist, also consistent with lower energy barriers for the Rây−Dutt mechanism. We also observe that, as b increases within our series from Sc^{III} ($b = 1.31$) < Ti^{IV} ($b = 1.33$) < Zn^{II} ($b = 1.39$), < Ga^{III} ($b = 1.43$), Ge^{IV} ($b = 0.46$), the relative differences in the activation barriers between the Bailar and Rây−Dutt mechanisms increase: Sc^{III} ($\Delta\Delta G^{\ddagger} = 0.4$ kcal mol^{-1}) < Ti^{IV} ($\Delta\Delta G^{\ddagger} = 0.8$ kcal mol^{-1}) ~ Zn^{II} ($\Delta\Delta G^{\ddagger} = 0.8$ kcal mol^{-1}) < Ga^{III} ($\Delta\Delta G^{\ddagger} = 1.3$ kcal mol^{-1}) < Ge^{IV} ($\Delta\Delta G^{\ddagger} = 2.5$ kcal mol^{-1}), again consistent with theoretical predictions. Within our series of examined complexes of the mda ligand, a comparison of b, d_{A-A}/l_{A-A}, and $\Delta\Delta G^{\ddagger}$ values correctly predicts the general trends; however, our results suggest that the Zn(mda)$_3^-$ monoanion should have a higher barrier than what we have found computationally. Our computed activation barrier for the Zn^{II} complex is closer to that of the Sc^{III} or Ti^{IV} complex, although the value of b is more similar to that of our Ga^{III} complex. Ligand−ligand repulsions increase as the charge on the complex increases[3] and should favor distortion toward octahedral geometry, which would also *increase* (rather than decrease) the barrier for an intramolecular rearrangement that proceeds via a trigonal-prismatic transition state. Furthermore, Raymond et al. propose that complexes with filled or partially filled d orbitals should not favor distortion toward

the trigonal-prismatic transition state, which would lower the activation barrier.[11] We do not understand at this point why the computed activation barriers for intramolecular rearrangements in Zn(mda)$_3^-$ are so low.

Conclusions

The original suggestions for two different dynamic processes for the nondissociative ligand permutation in some octahedral transition-metal complexes were made more than half a century ago. Arguments have been put forward that suggest that the preferred pathway can be predicted by calculating either the normalized bite or the ratio of the donor-to-donor atom distance within one chelate to the donor-to-donor atom distance of donor atoms in adjacent chelates (d_{A-A}/l_{A-A}). Theory predicts that metal trischelate complexes with a normalized bite above 1.3 should favor a Rây−Dutt twist over a Bailar twist intramolecular rearrangement and that complexes with d_{A-A}/l_{A-A} ratios near 1 (as is the case for all of our model complexes in this study; see Table 4) should show only a small preference for racemization via one pathway over the other. Our computational study is consistent both with these theoretical predictions and within the trends of experimentally observed data for several metal−ligand complexes. We find (a) that Sc(mda)$_3$, [Ti(mda)$_3$]$^+$, and [Zn(mda)$_3$]$^-$ should be highly fluxional molecules, with low barriers to Δ and Λ interconversion, (b) that across the series of mda complexes from Sc^{III} to Ge^{IV} the Rây−Dutt energy is consistently, but only slightly, lower than that of the Bailar process, and (c) that the barriers for intramolecular rearrangement increase as the normalized bite increases within this same series, which is also consistent with experimental observations. We also find (d) that the dynamic process for Co(mda)$_3$ specifically involves dissociative exchange via a five-coordinate Co^{III} intermediate (more precisely, this is probably an intermediate on the total energy potential surface and, more speculatively, with a transition state for dissociation existing only on the free-energy potential surface). This is consistent with experimental observations for the tris-β-diketonates of Co^{III} and consistent with our finding that the computed barriers for intramolecular rearrangement in Co(mda)$_3$ are significantly higher than those available through the dissociative mechanism.